

Fig. 4-28(a) the $I_{DS}-V_{GS}$ curves of poly-Si TFT with main grain boundary in the channel (GB device) without LDD

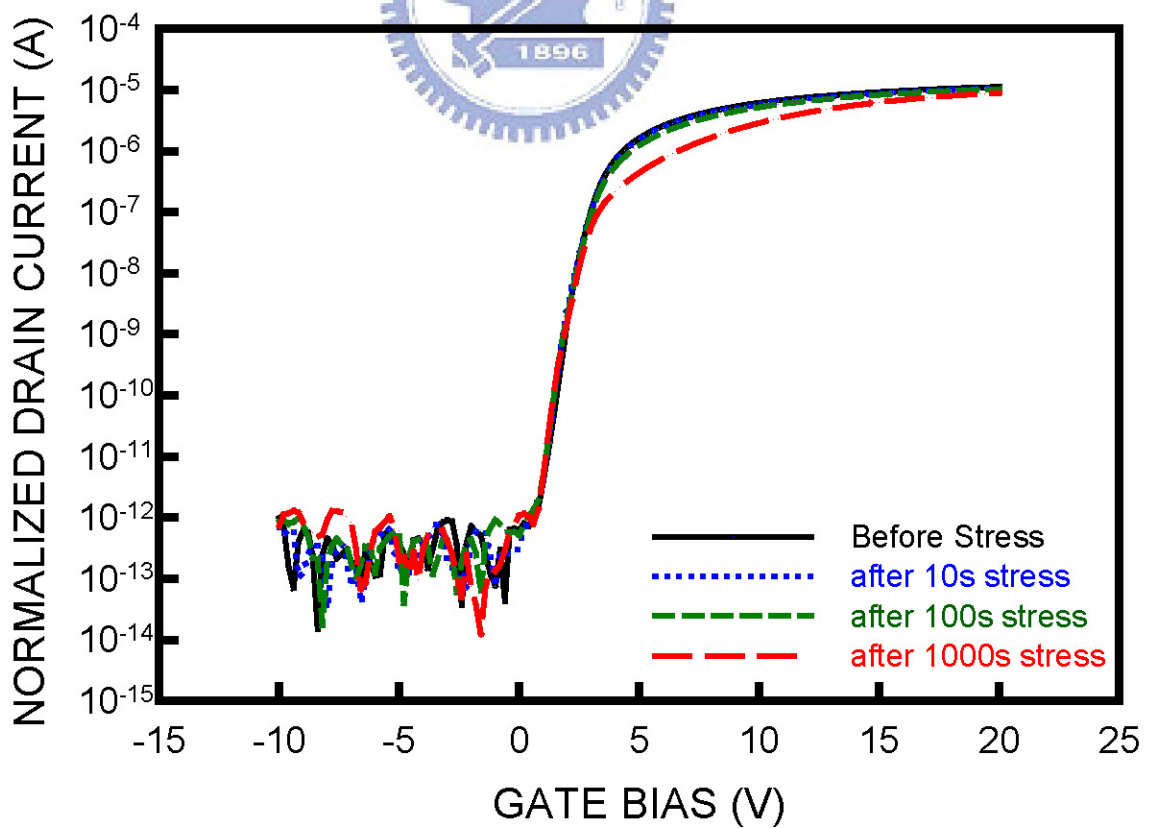


Fig. 4-28(b) the $I_{DS}-V_{GS}$ curves of poly-Si TFT without main grain boundary in the channel (NGB device) without LDD

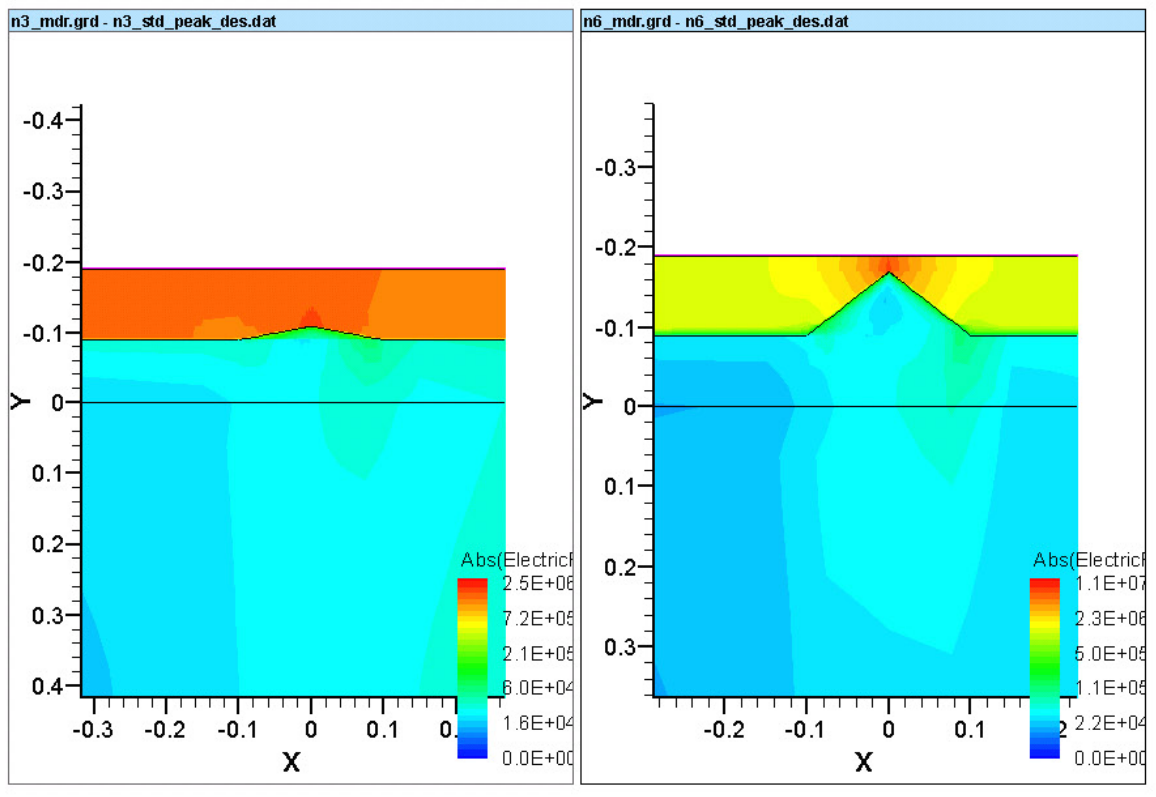


Fig. 4-29 the electrical field simulation of NGB and GB at gate oxide interface, the left is NGB, and the right is GB

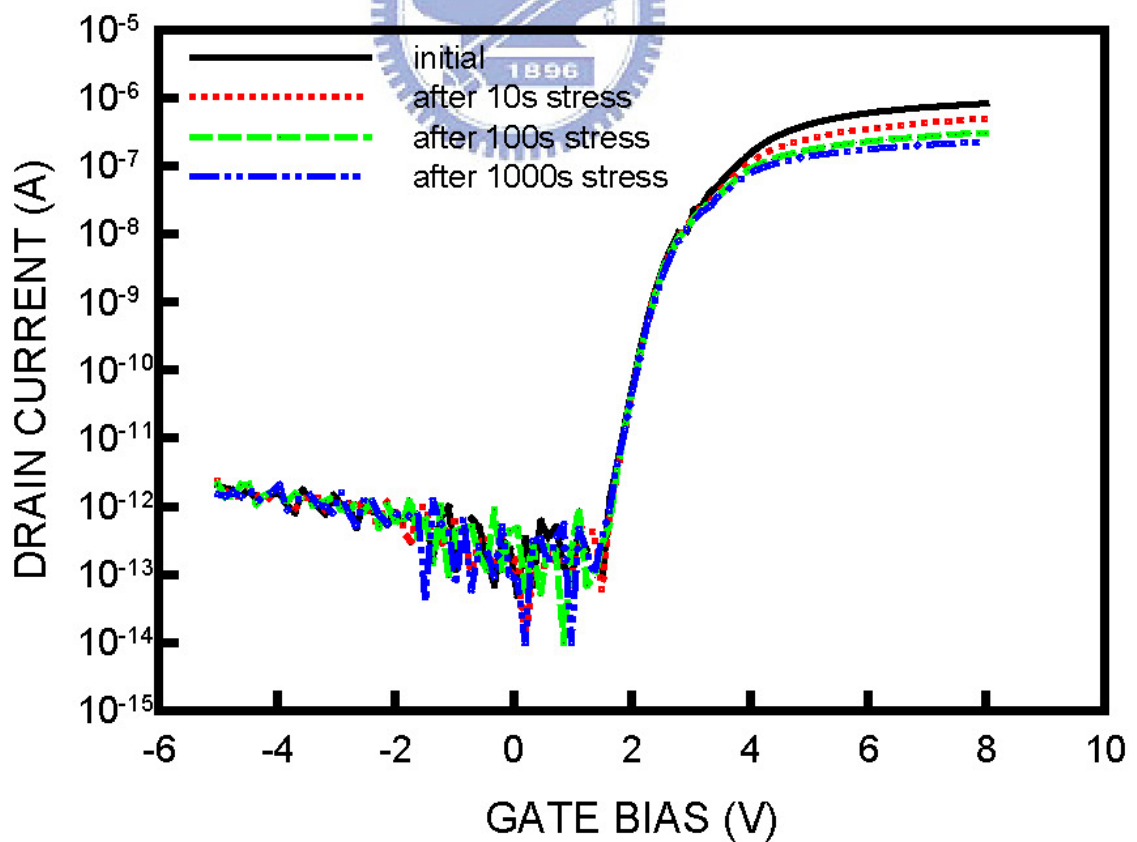


Fig. 4-30(a) the $I_{DS}-V_{GS}$ curves of poly-Si TFT without main grain boundary in the channel (NGB device) with $1.0 \mu\text{m}$ LDD LDD

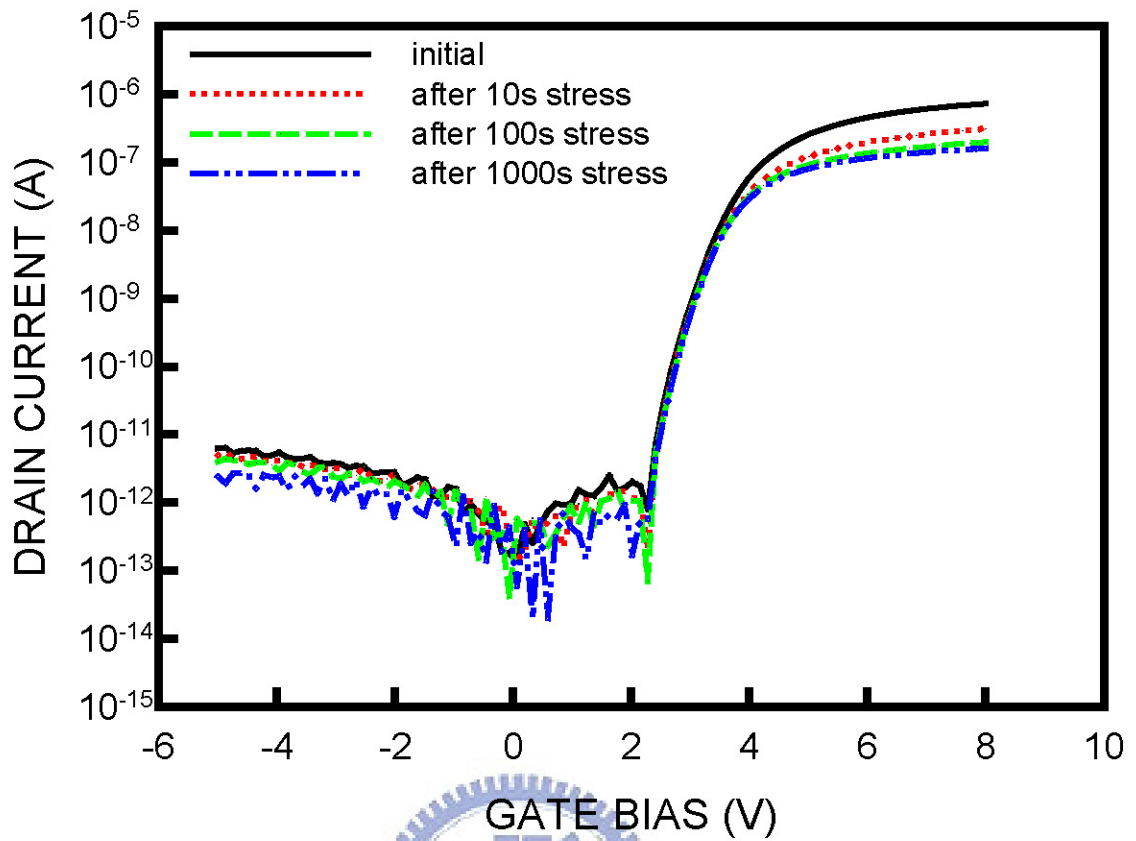


Fig. 4-30(b) the I_{DS} - V_{GS} curves of poly-Si TFT with main grain boundary in the channel (GB device) with $1.0 \mu\text{m}$ LDD LDD

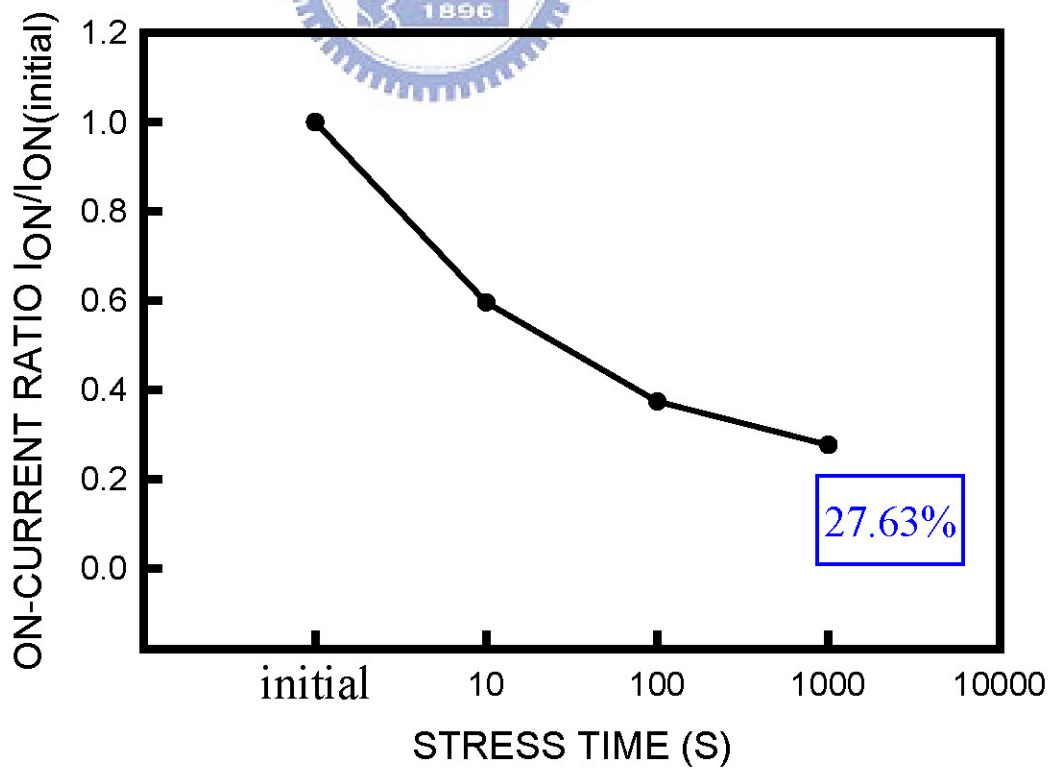


Fig. 4-31(a) the degraded on-current ratio versus stress time curve of an NGB TFT with $1.0 \mu\text{m}$ LDD at $V_{DS}=0.1\text{V}$

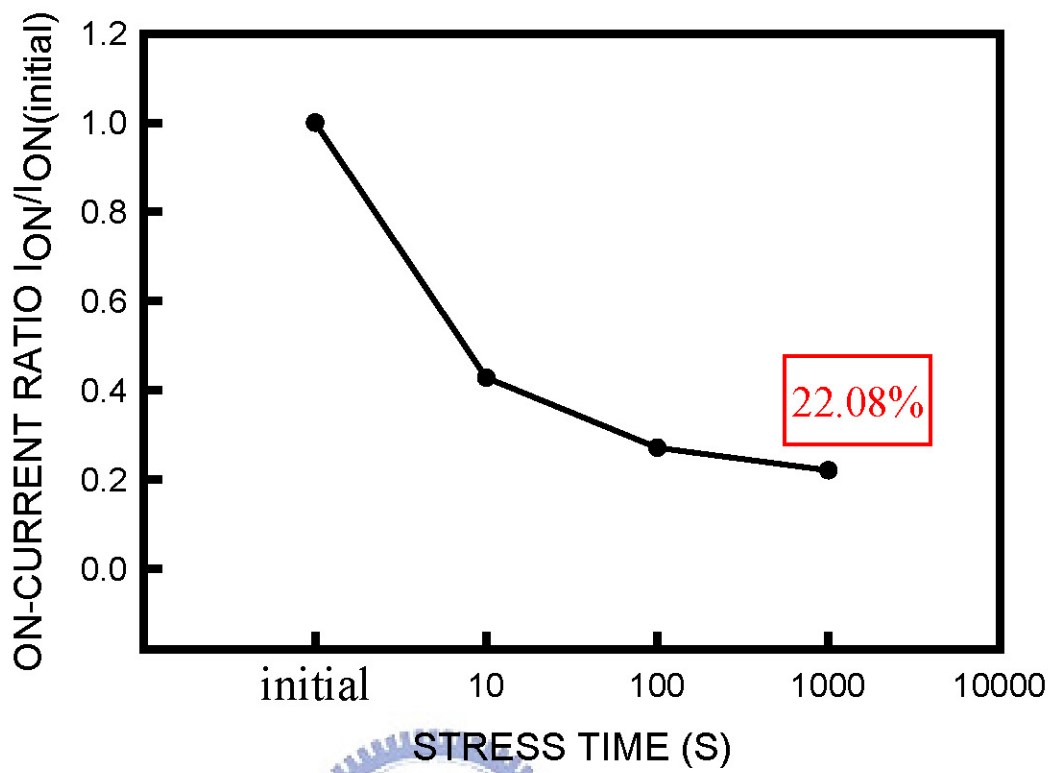


Fig. 4-31(b) the degraded on-current ratio versus stress time curve of an GB TFT with $1.0 \mu\text{m}$ LDD at $V_{DS}=0.1\text{V}$

